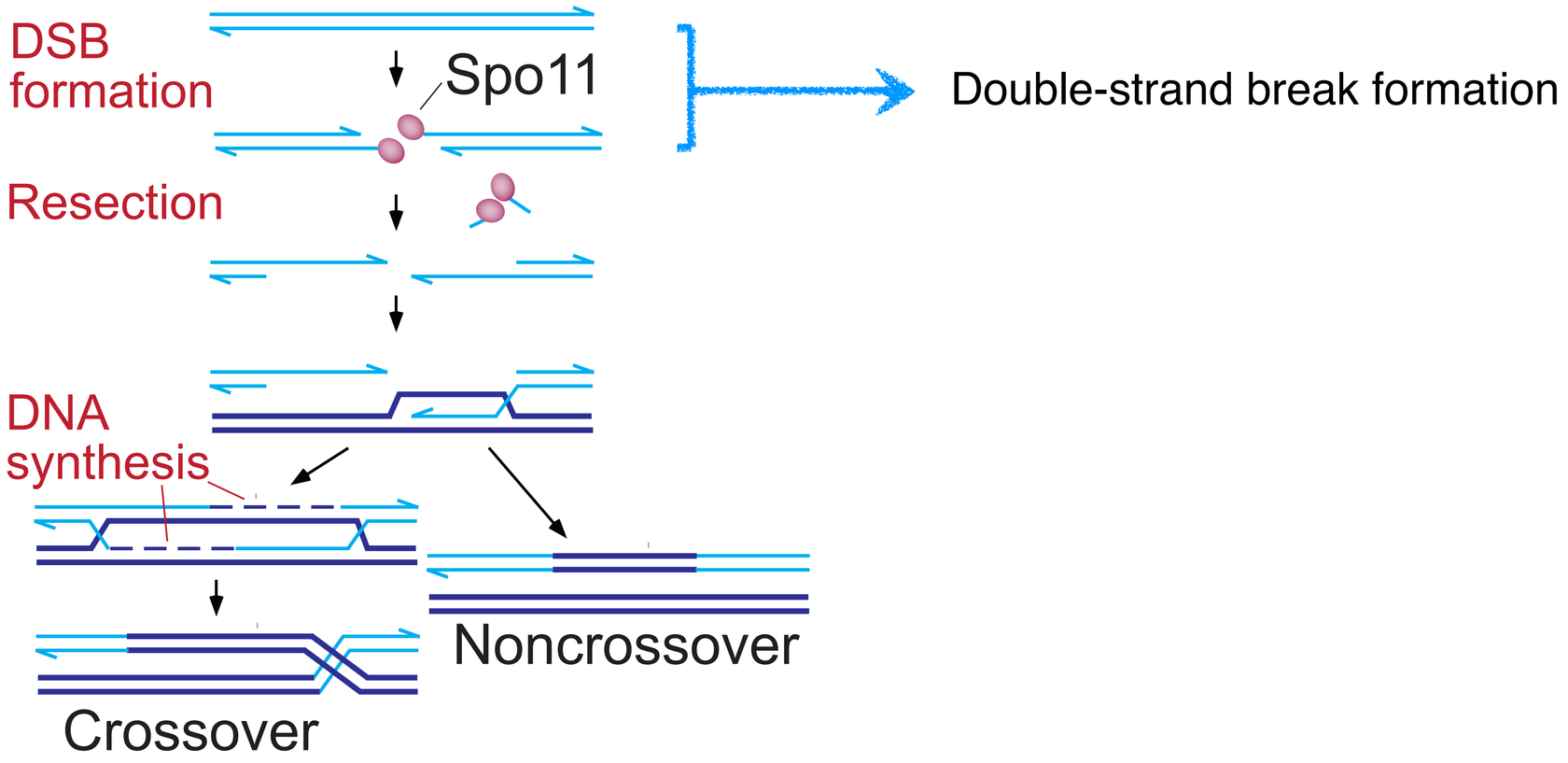
DSB
formation
Spo11
Double-strand break formation
Resection
DNA
synthesis
Noncrossover
Crossover

Meiosis-Specific DNA Double-Strand Breaks Are Catalyzed by Spo11, a Member of a Widely Conserved Protein Family

Scott Keeney,* Craig N. Giroux,† and Nancy Kleckner*
*Department of Molecular and Cellular Biology
Harvard University
Cambridge, Massachusetts 02138
†Center for Molecular Medicine and Genetics
Wayne State University
Detroit, Michigan 48202

1997
PMID: 9039264

An atypical topoisomerase II from archaea with implications for meiotic recombination

Agnès Bergerat, Bernard de Massy, Danielle Gadelle, Paul-Christophe Varoutas, Alain Nicolas & Patrick Forterre

1997, PMID: 9121560

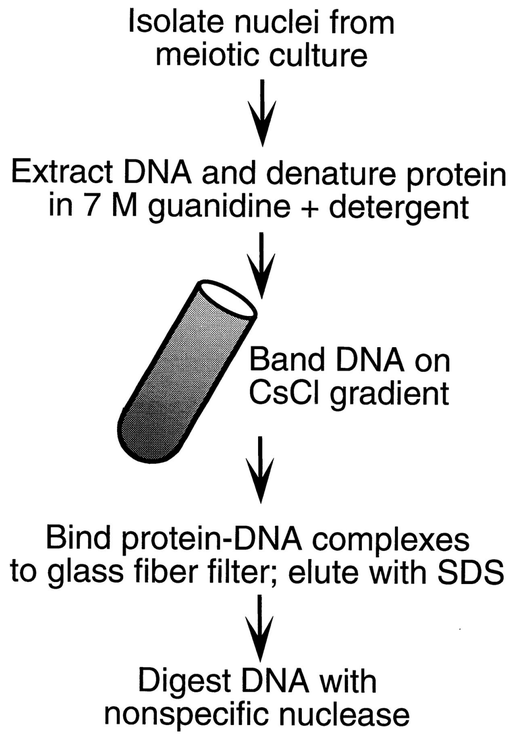

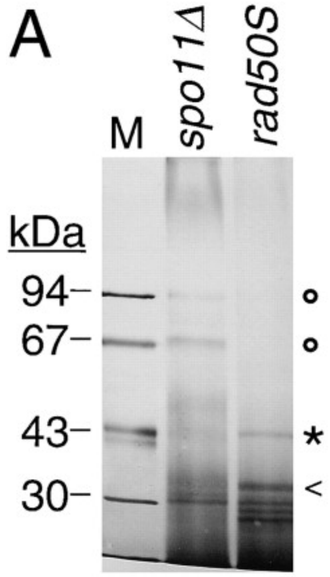

DSB-forming machinery: The (mostly) conserved parts list

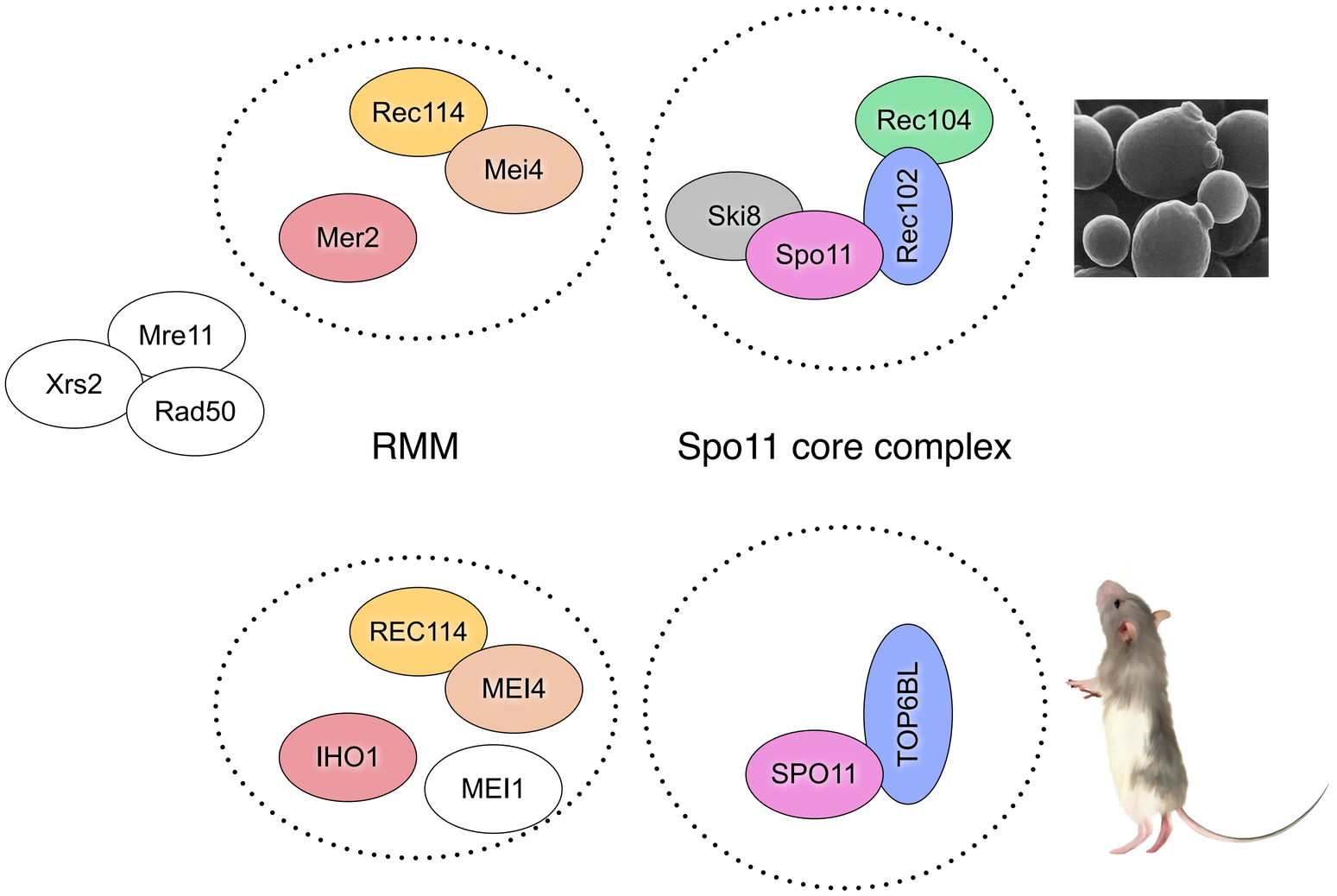

Spo11 is related to archaeal topoisomerase VI

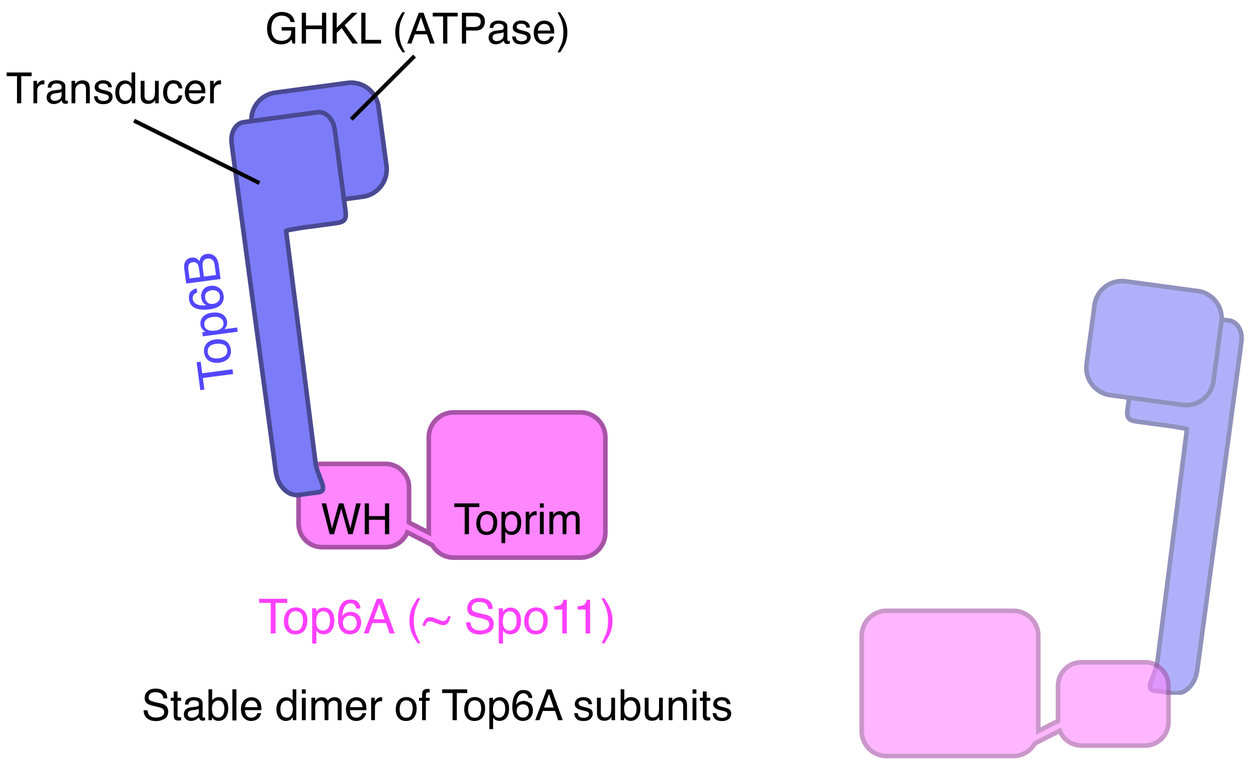

Berger & Forterre labs; figures adapted from
Corbett & Berger, 2007, PMID: 17603498

Spo11 is related to archaeal topoisomerase VI

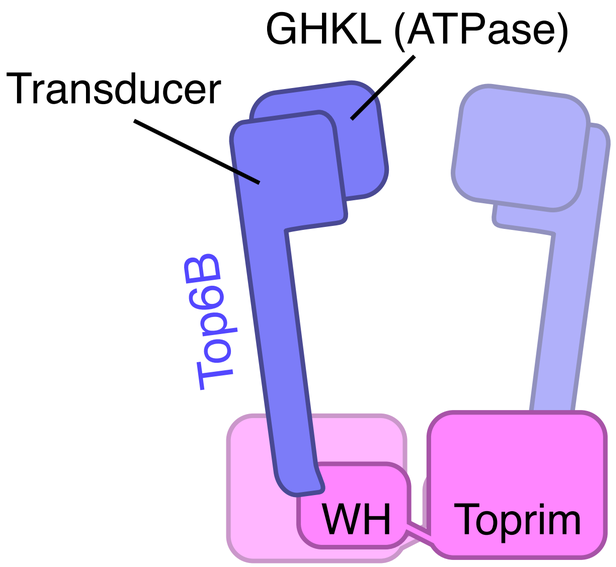

Top6A (~ Spo11)

Stable dimer of Top6A subunits

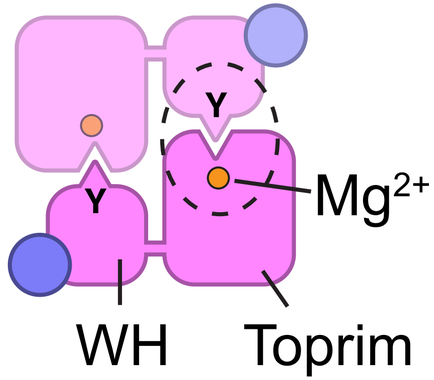

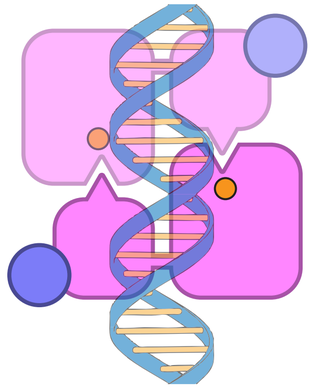

Berger & Forterre labs; figures adapted from
Corbett & Berger, 2007, PMID: 17603498

Purification of distinct Rec114–Mei4 and Mer2 complexes

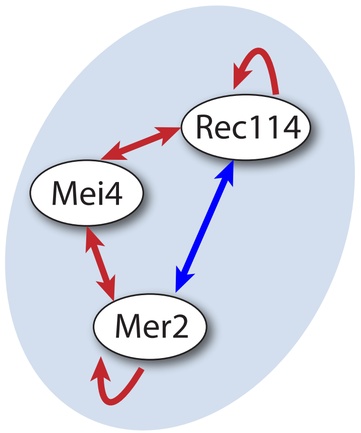

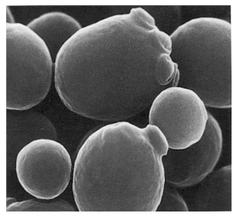

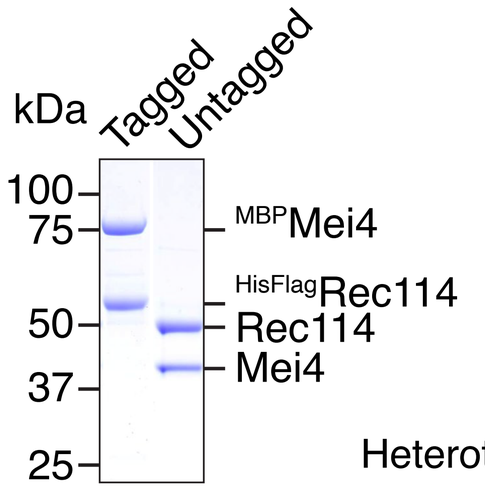

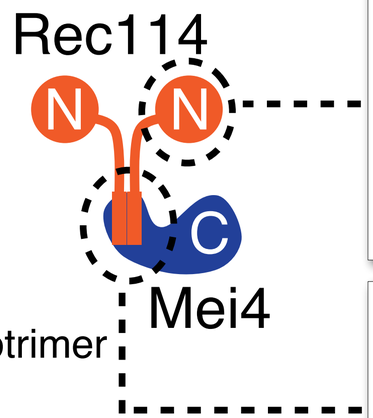

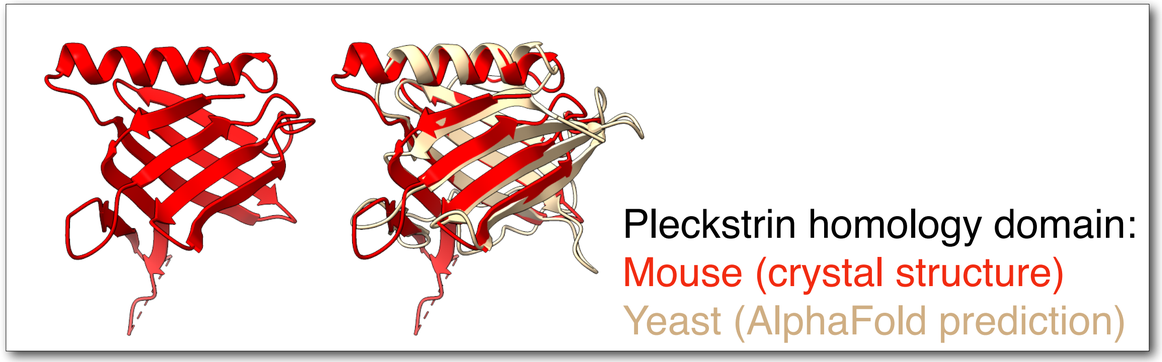

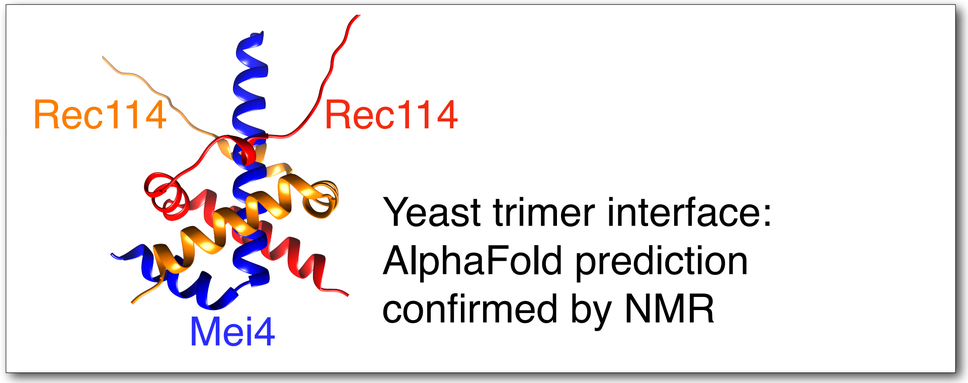

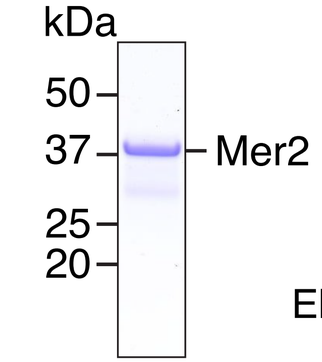

Elongated homotetramer

*Claeys Bouuaert, Keeney et al., 2021, PMID: 33731927

Kumar, de Massy, Kadlec et al., 2018, PMID: 30569039
*Boekhout, Patel, Keeney et al., 2019, PMID: 31003867
*Liu, Eliezer, Keeney et al., 2023, PMID: 37442580
Daccache, Claeys Bouuaert et al., 2023, PMID: 37442581

Rec114–Mei4 and Mer2 assemble cooperatively on DNA

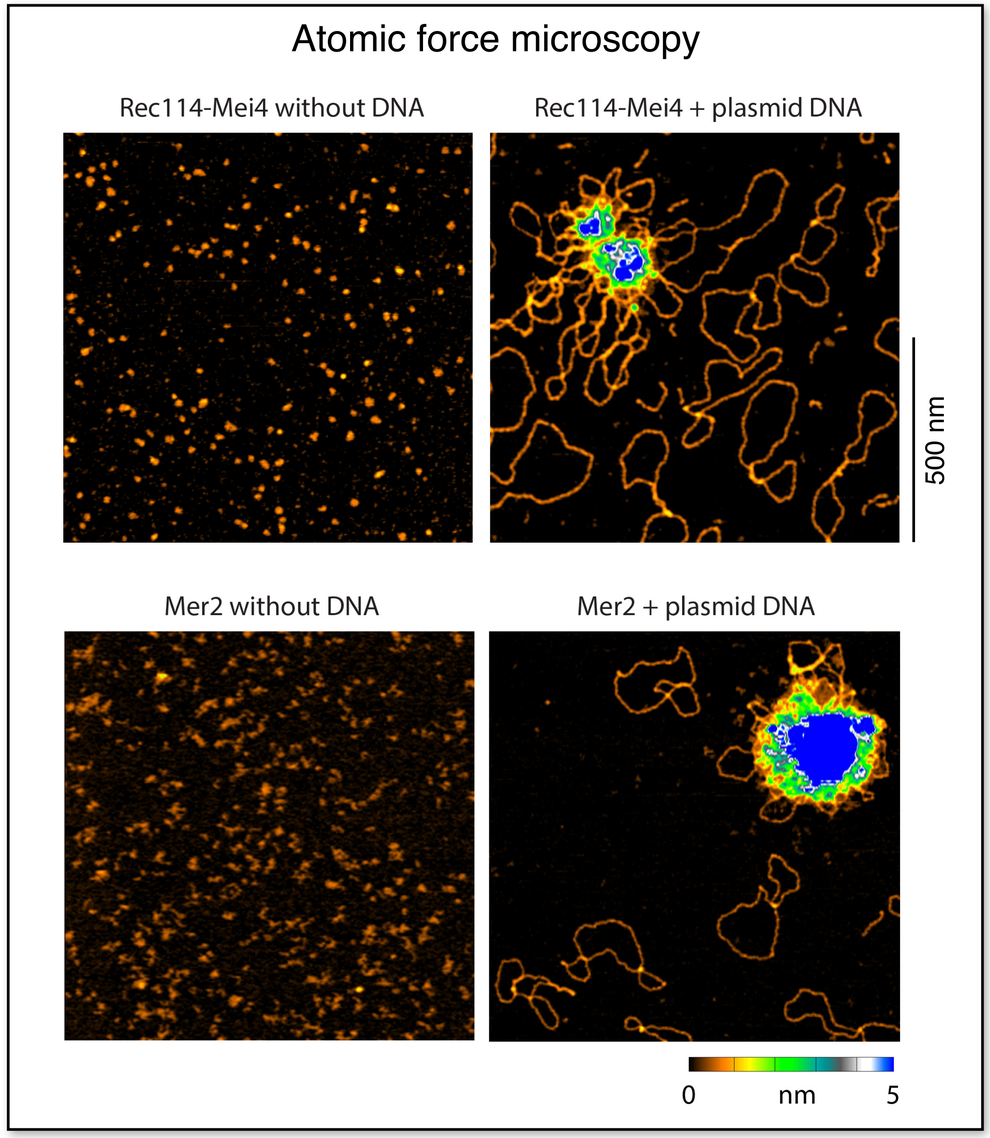

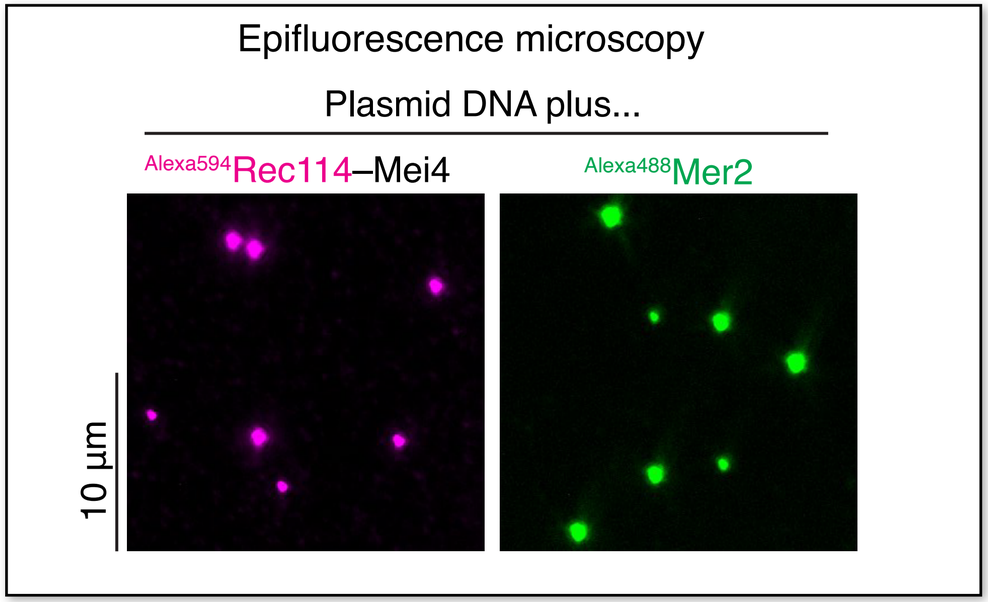

- ✓ Promoted by molecular crowding (polyethylene glycol)
- ✓ Reversible (challenge with high salt, DNase I)
- ✓ Can fuse
  - ➢ Reminiscent of **phase separation** systems.
- ✓ Mutations that weaken DNA binding:
  - disrupt condensate formation in vitro
  - disrupt RMM function in vivo

*Claeys Bouuaert, Keeney et al., 2021, PMID: 33731927

RMM co-condensates recruit Spo11

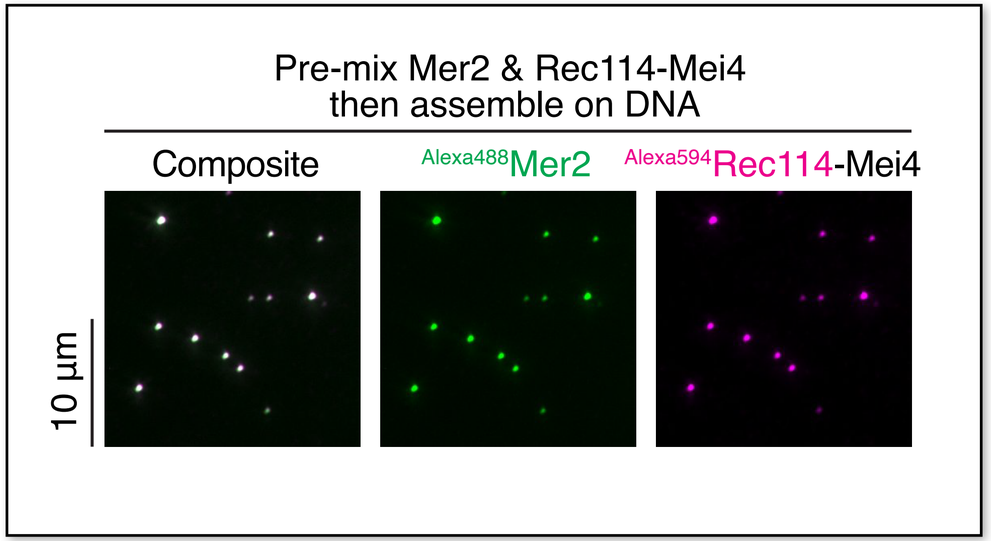

Rec114–Mei4 and Mer2
form stoichiometric
mixed condensates on DNA

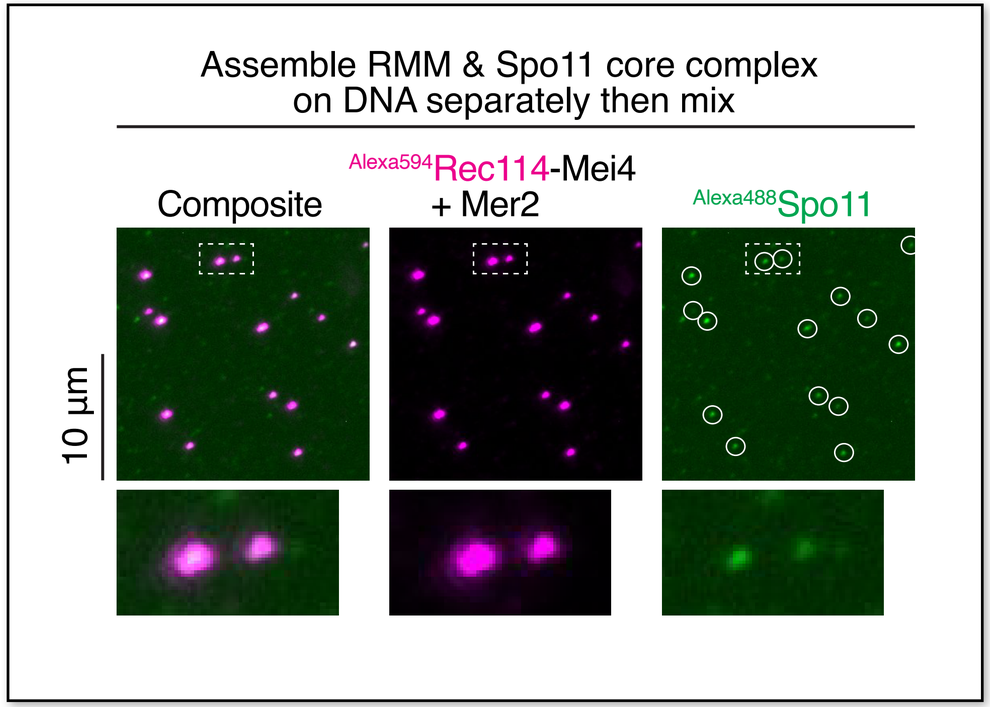

Joint RMM condensates
recruit Spo11 core complexes
via interactions with Rec102-Rec104

How to build (and control) a meiotic DNA-breaking machine

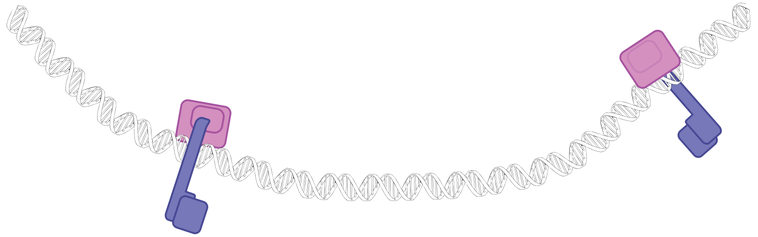

Feeble dimer formation and tight DNA binding create a kinetic trap that restrains SPO11 activity by keeping most of the DNA-bound protein monomeric

*Claeys Bouuaert, Keeney et al., 2021, PMID: 33731927
*Zheng, Keeney et al. 2024, PMID: 39605552

Assembly of the complete DSB machinery:

* Facilitates dimer formation by co-orienting and concentrating SPO11 complexes
* Ensures — via clustering — that the ensemble is an efficient DSB generator even if individual SPO11 complexes are not
* Controls when and where SPO11 is active

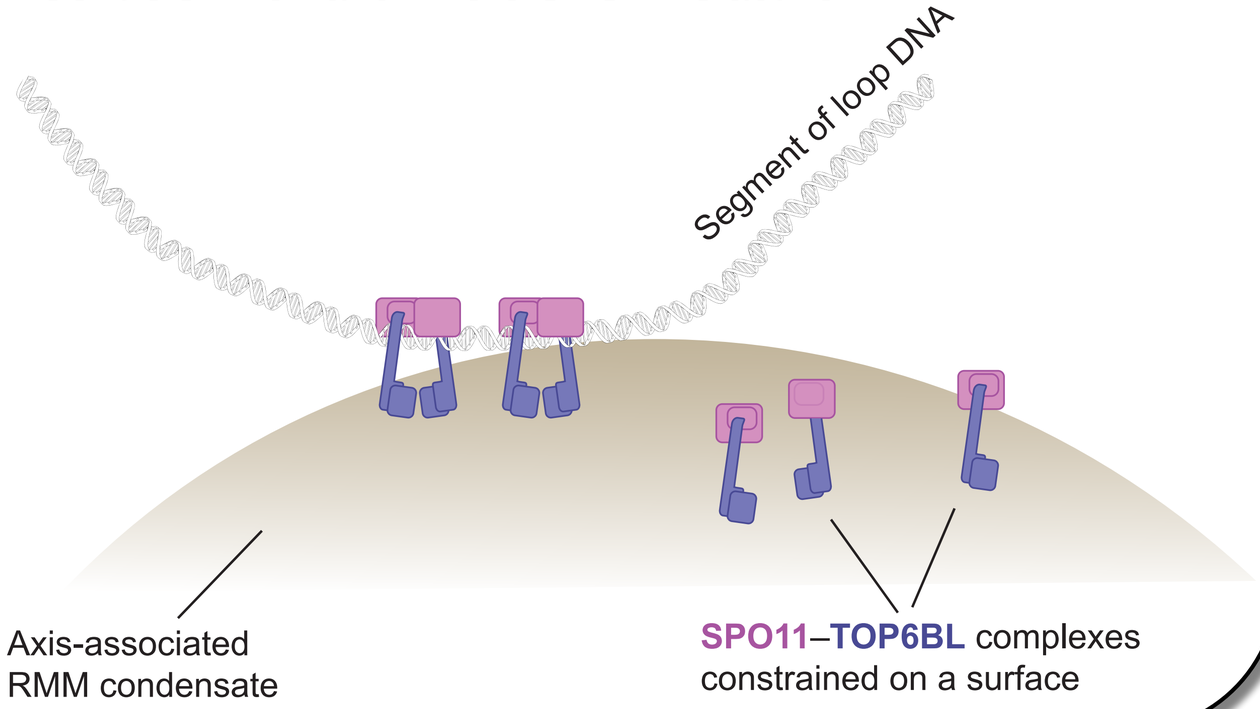

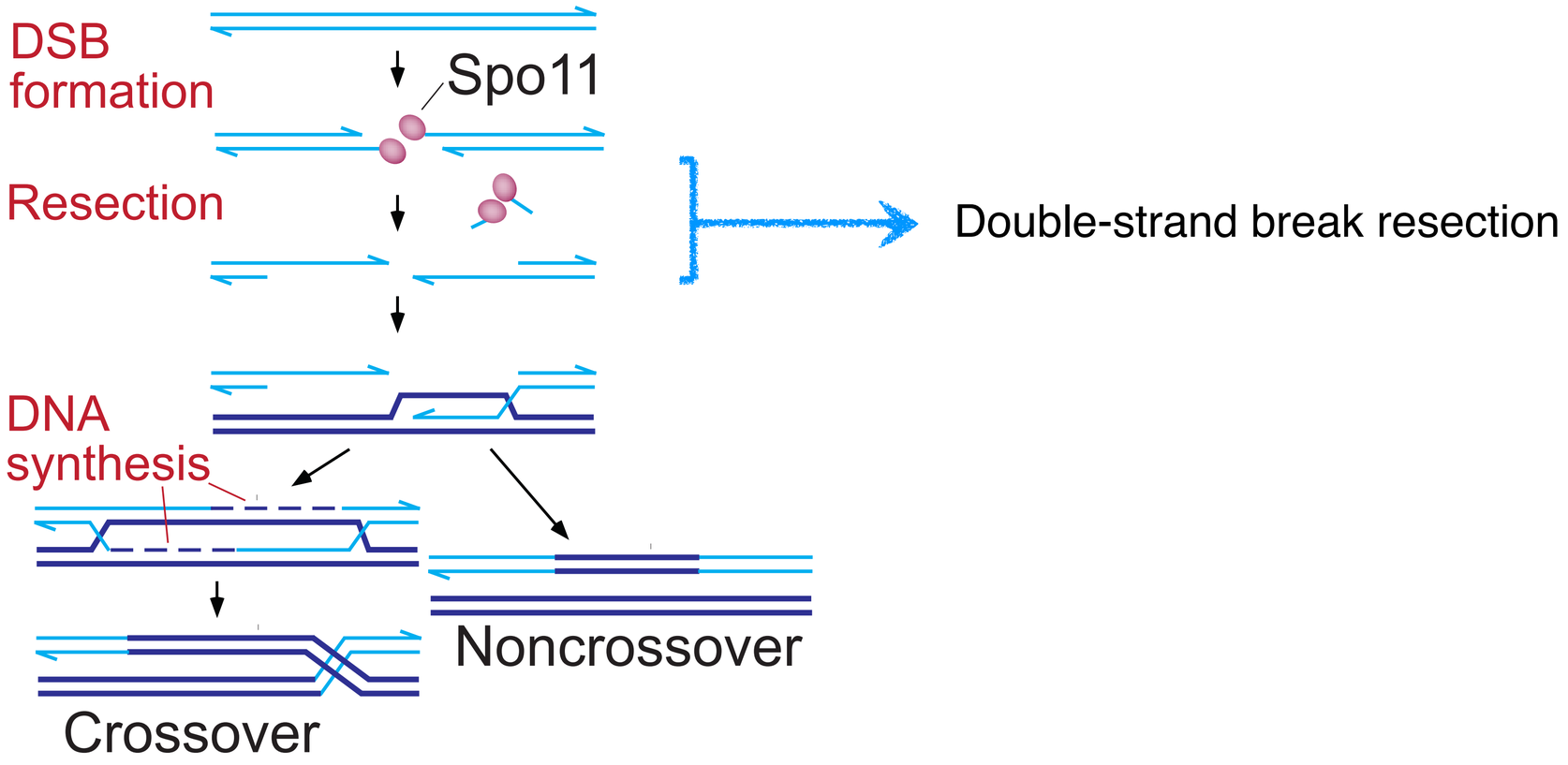
DSB
formation
Spo11
Resection
Double-strand break resection
DNA
synthesis
Noncrossover
Crossover

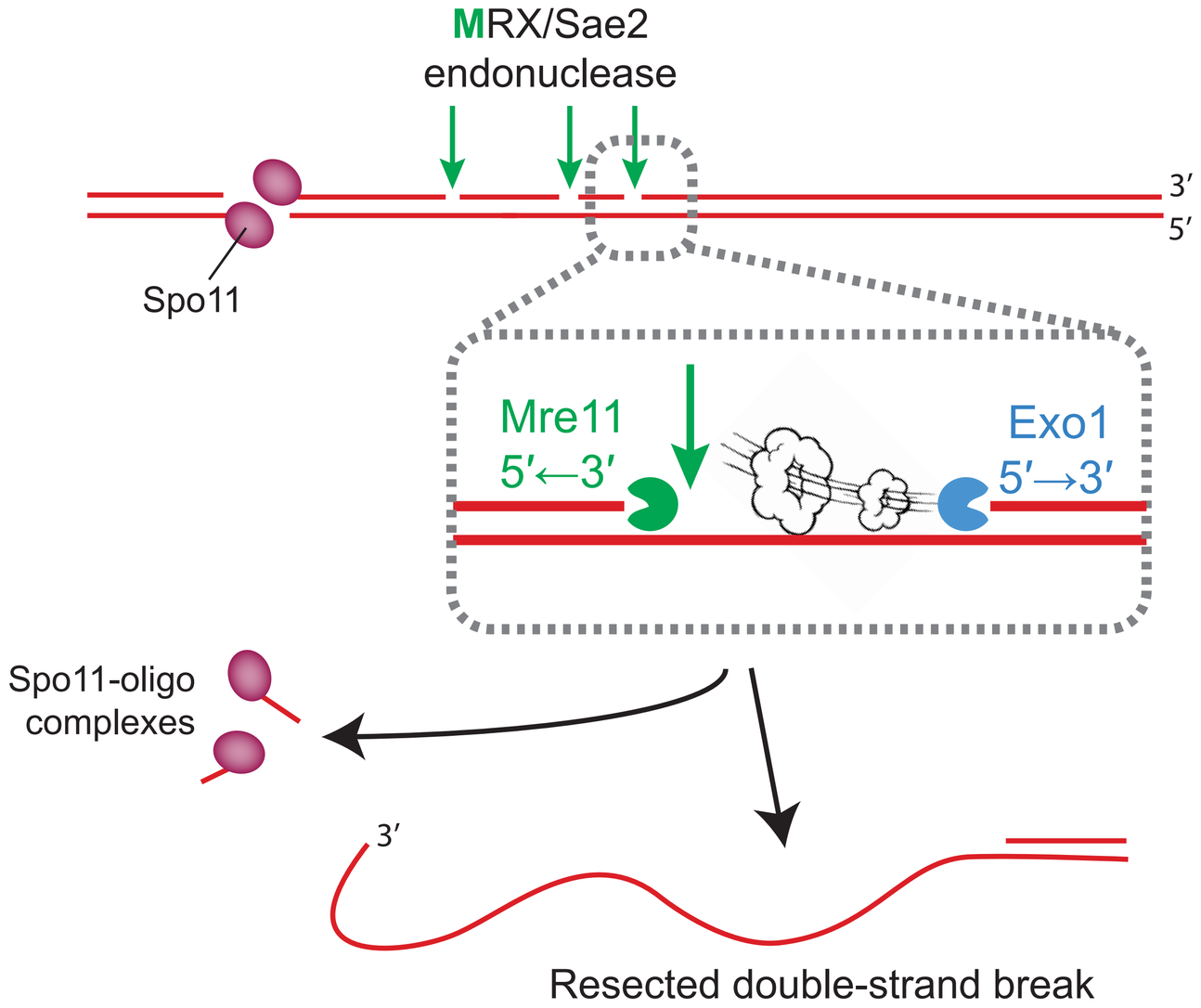
MRX/Sae2
endonuclease
3′
5′
Spo11
Mre11
5′←3′
Exo1
5′→3′
Spo11-oligo
complexes
3′
Resected double-strand break

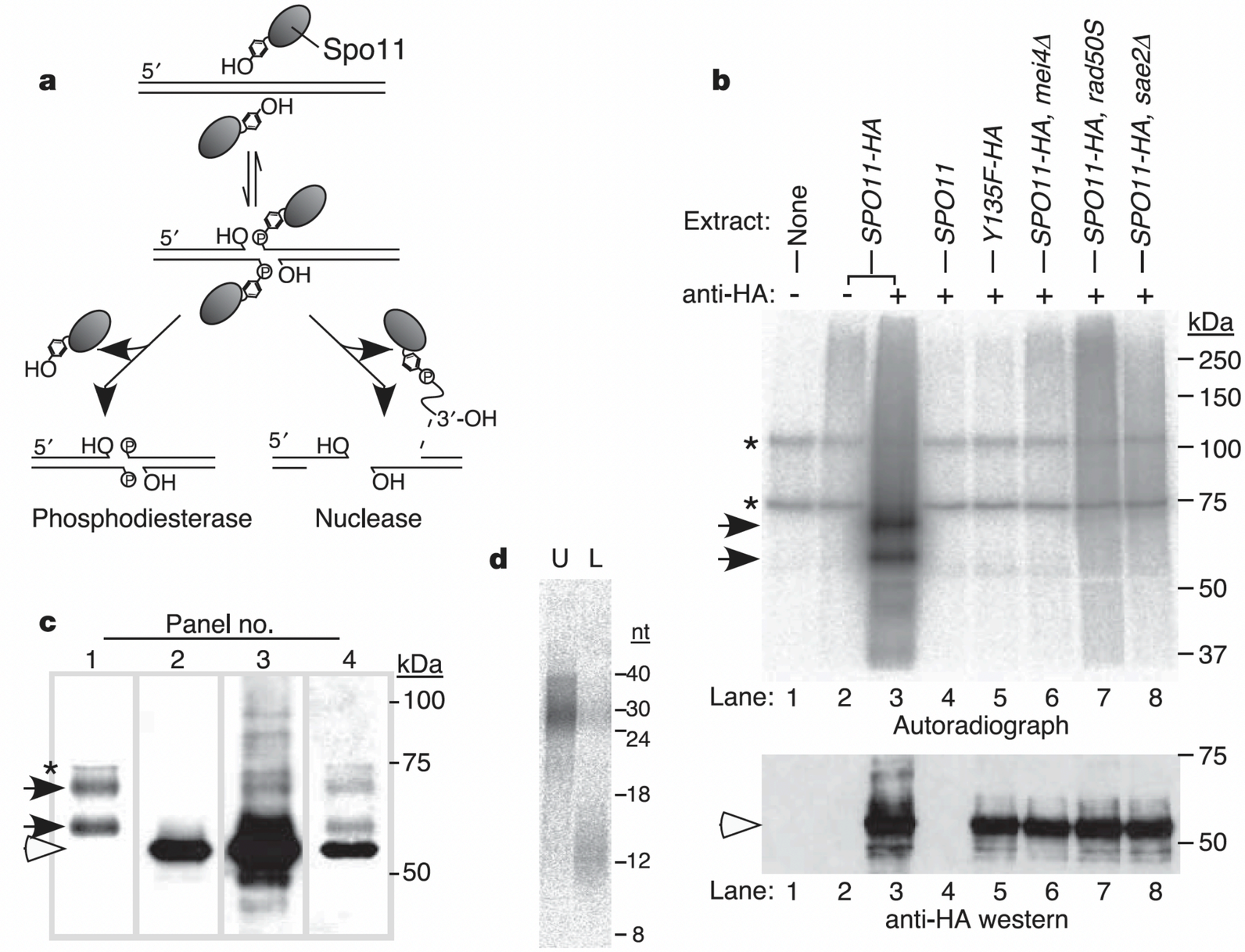

Neale, Pan & Keeney 2005, PMID 16107854

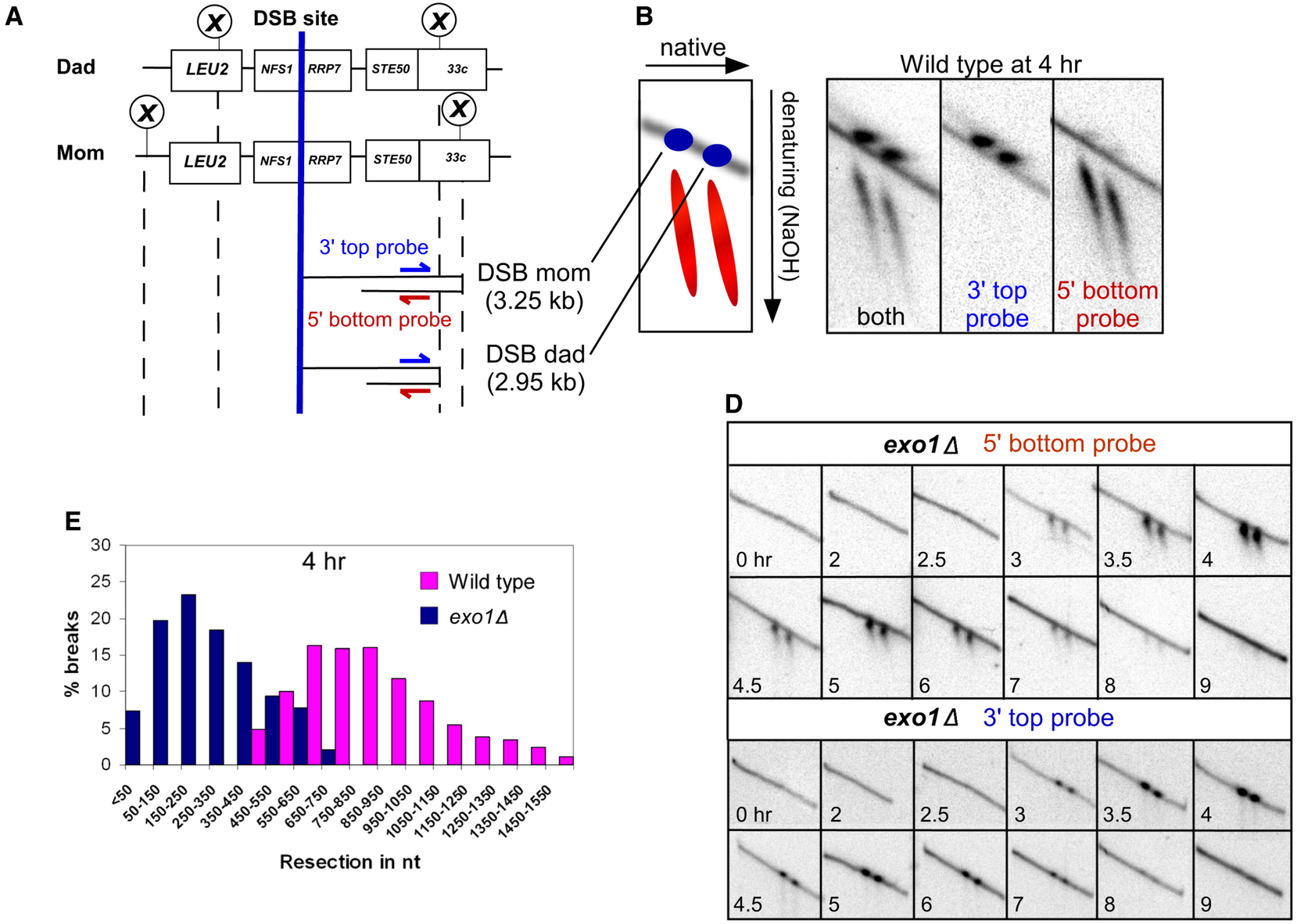

Zakharyevich, Hunter *et al.* 2010, PMID 21172664

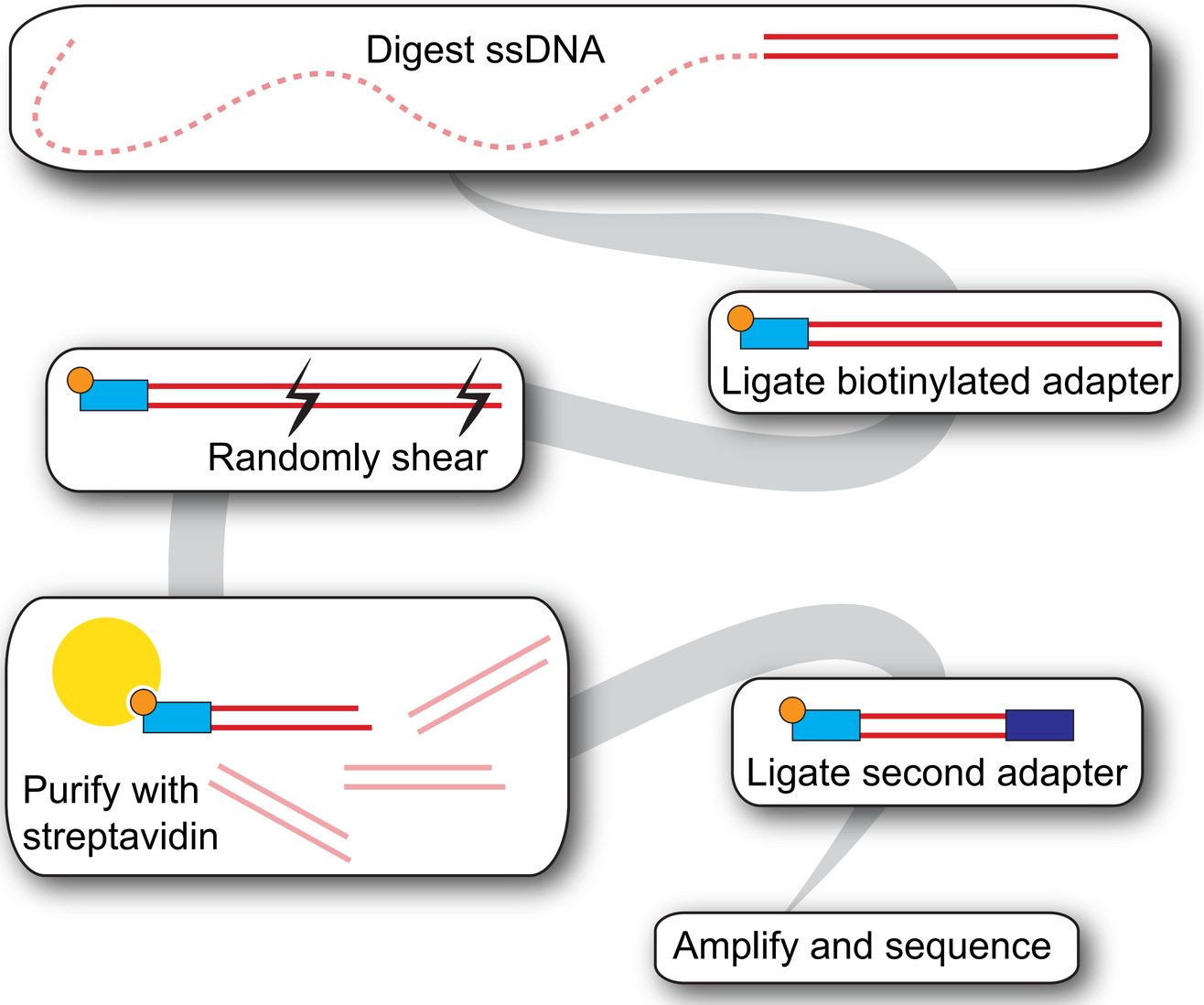

»S1 nuclease (S1-seq)

»ExoVII + ExoT (Exo7/T-seq)

»ExoT only (ExoT-seq)

Mimitou, Yamada & Keeney 2017 PMID 28059759
Yamada, Keeney et al. 2020 PMID 32354835
Paiano, Neussenzweig et al. 2020 PMID 32051414

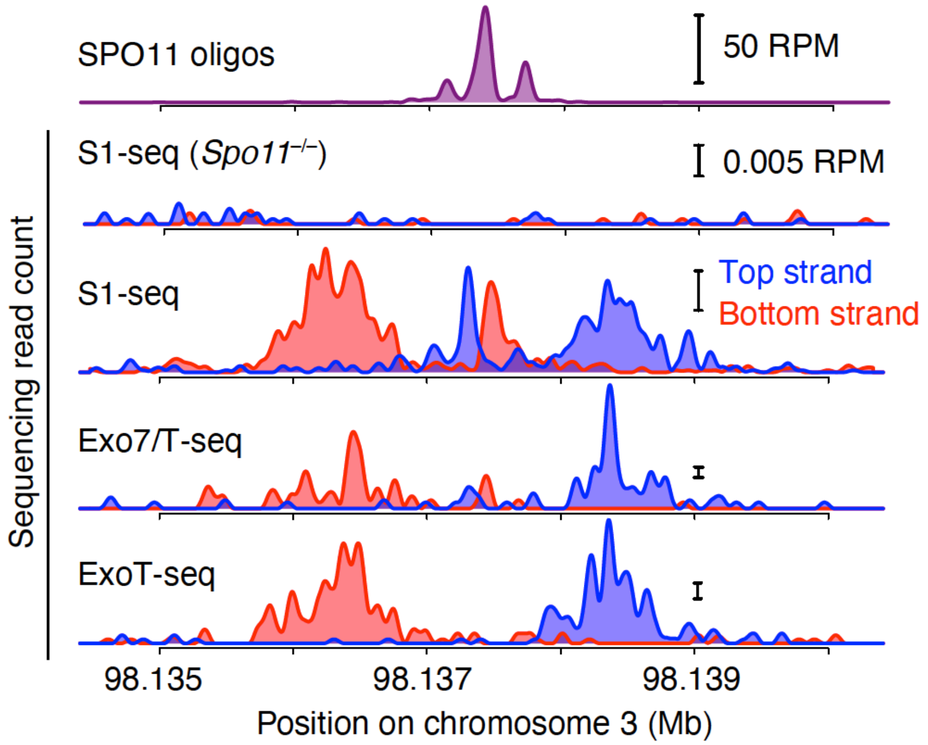

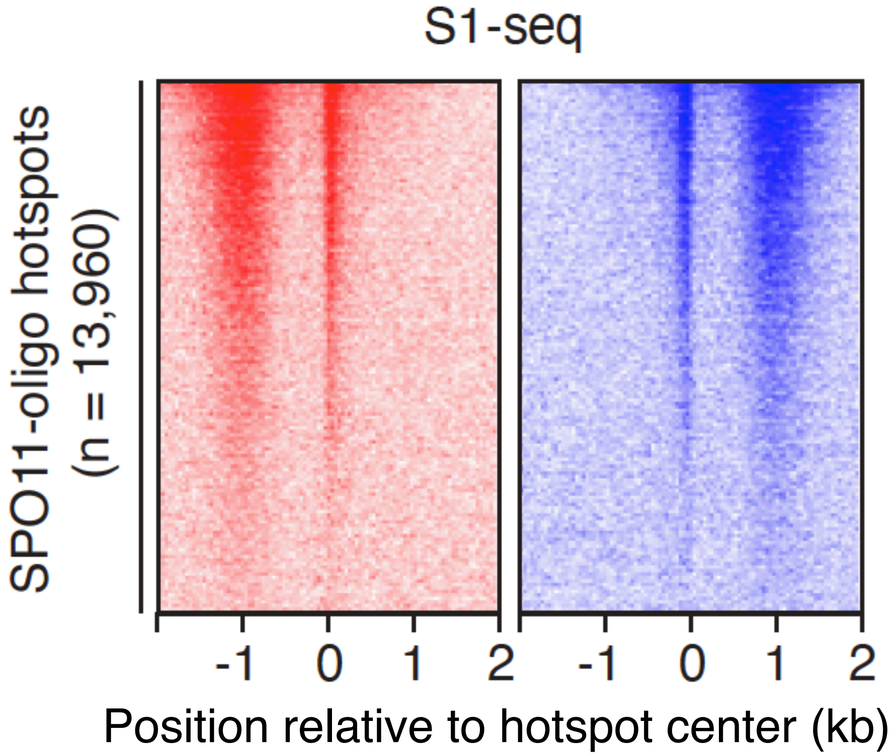

Kim, Keeney et al. 2025, PMID 40240347

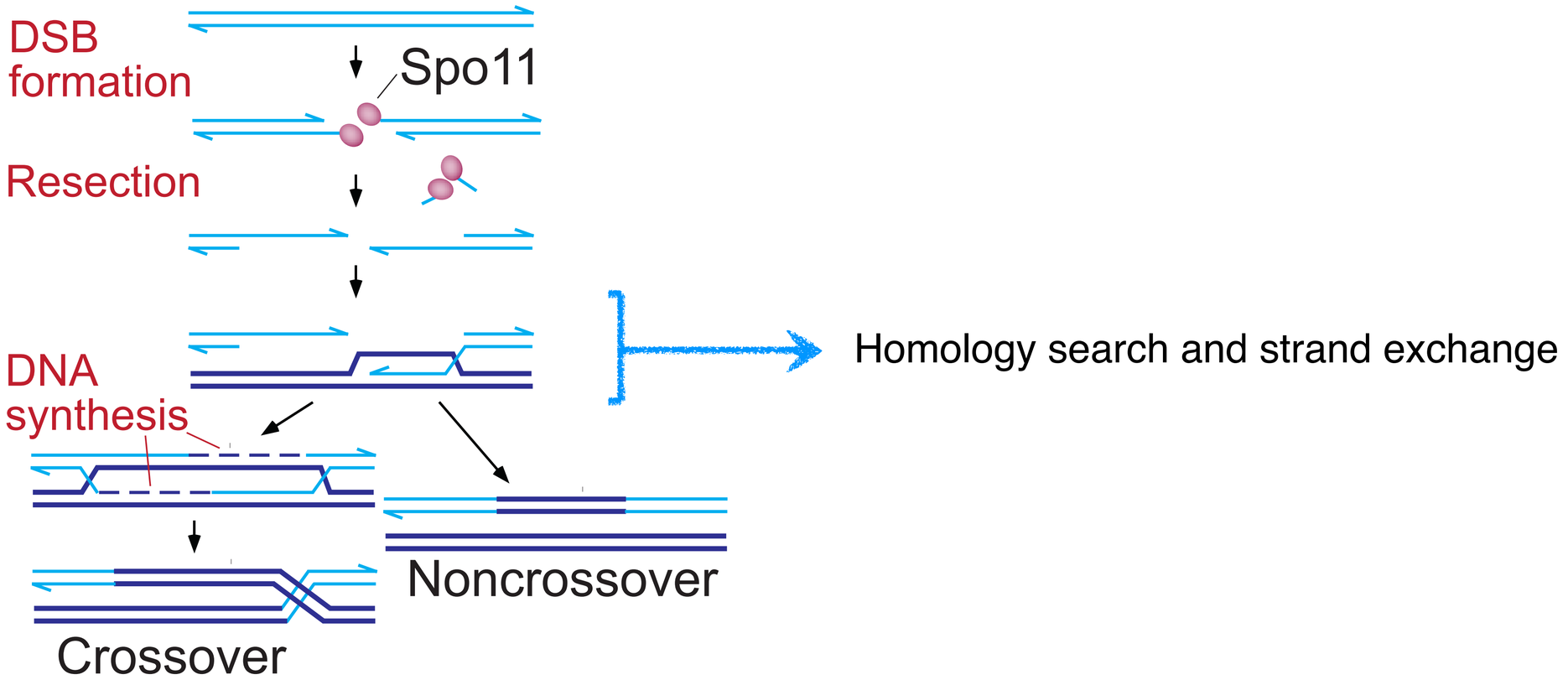
DSB
formation
Spo11
Resection
DNA
synthesis
Homology search and strand exchange
Noncrossover
Crossover

Homologous recombination

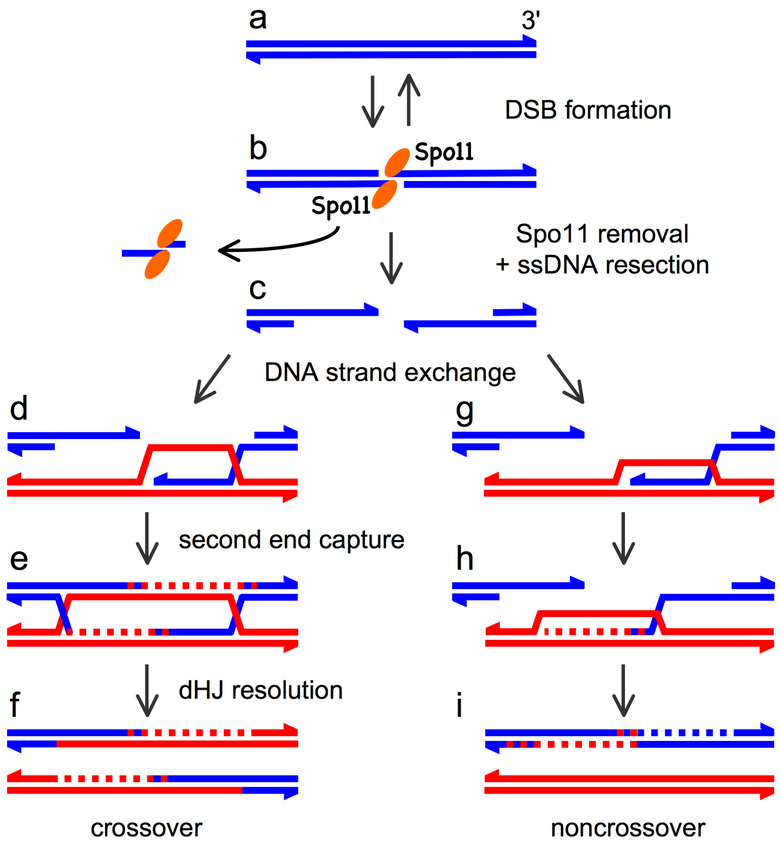

Examples of strand invasion and strand exchange reactions

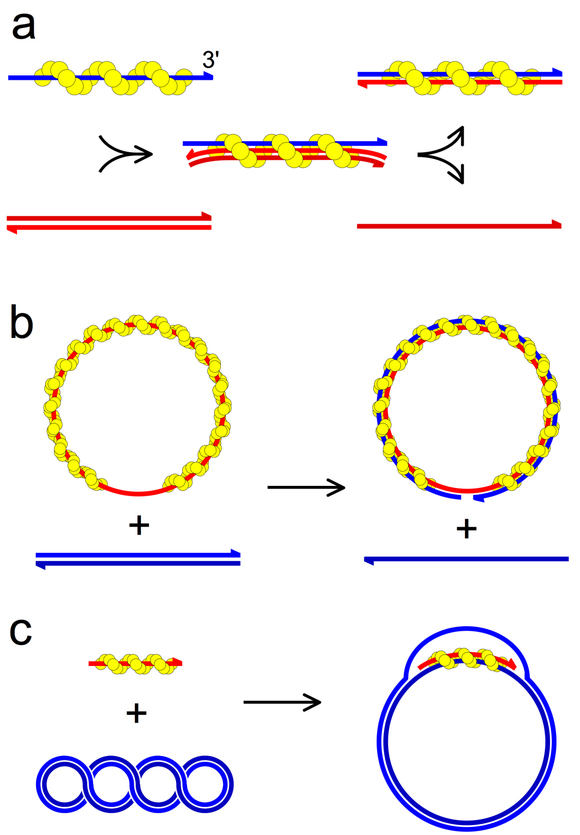

Figures from Neale & Keeney (2006) Nature 442: 153-8.

Electron micrograph of a RecA filament on ssDNA

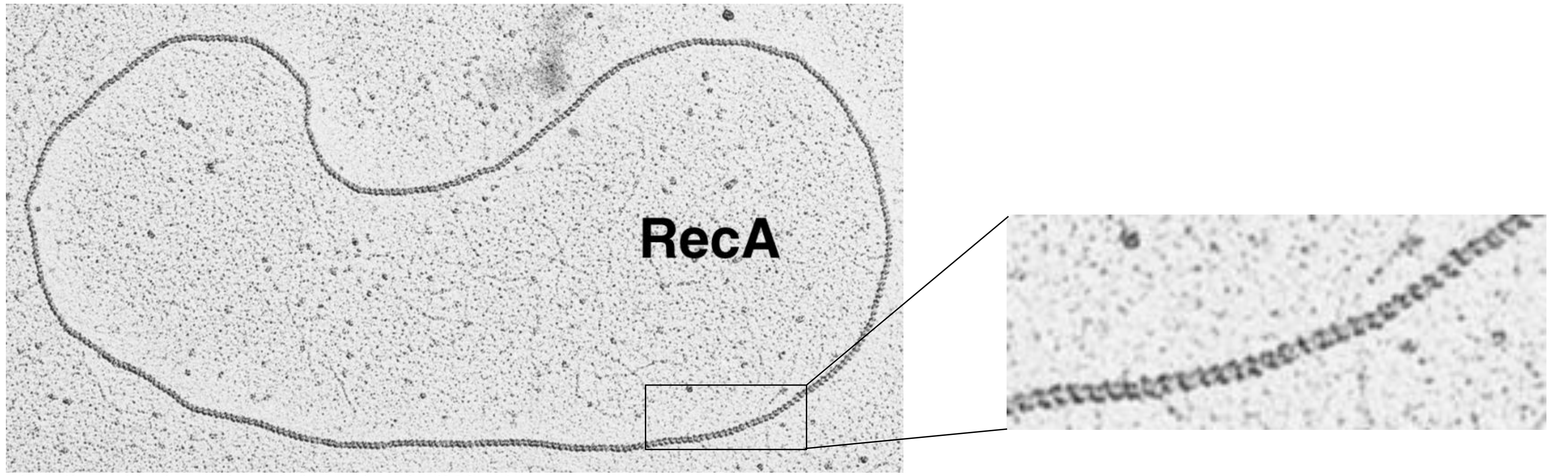

http://www.biochem.wisc.edu/inman/empics/0007a.jpg

Surface reconstructions
of filaments on ssDNA

99Å pitch
6.4 monomers/turn

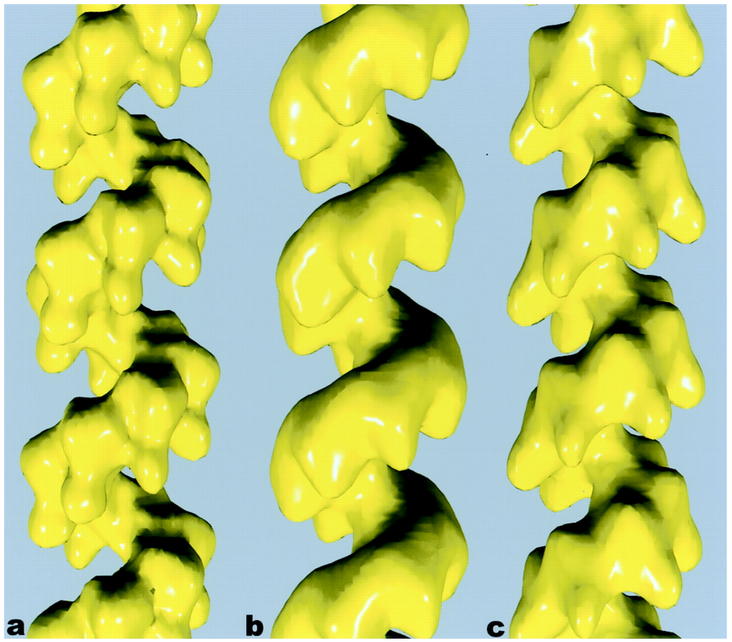

human
RAD51

Yeast
Rad51

E. coli
RecA

91Å pitch
6.2 monomers/turn

Yu et al. PNAS. 2001 98:8419-24.

Crystal structure of RecA nucleoprotein filaments

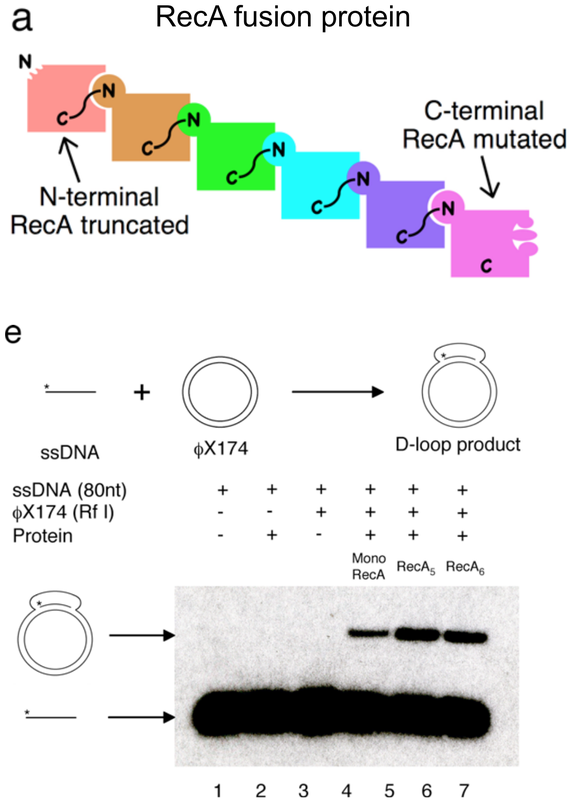

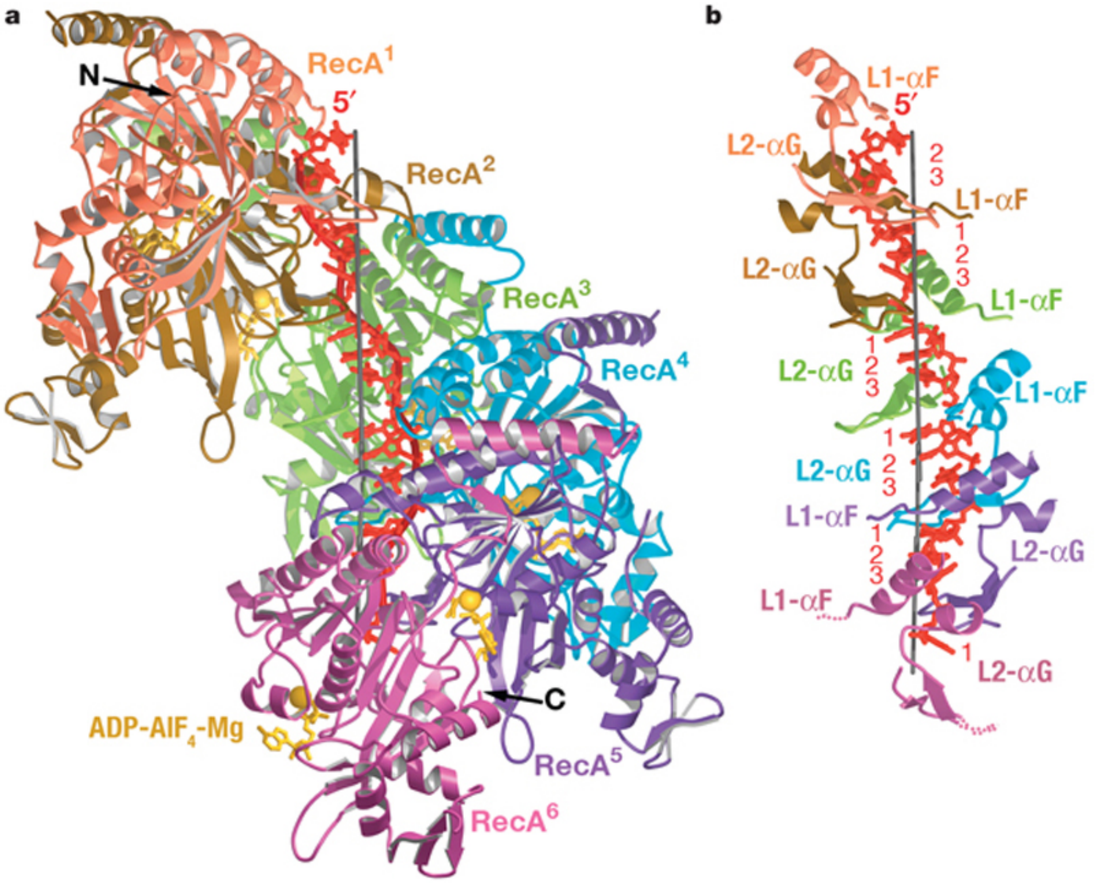

a, Structure of the $RecA_6$–$(ADP\text{-}AlF_4\text{-}Mg)_6$–$(dT)_{18}$ complex. The six RecA protomers are numbered from the N-terminal RecA of the fusion protein and are coloured pink, brown, green, cyan, purple and magenta, respectively. Only 15 of the 18 nucleotides are ordered (red). The DNA backbone is traced by a red coil. The six $ADP\text{-}AlF_4\text{-}Mg$ molecules are coloured gold. The five individual rotation/translation axes that relate adjacent RecA protomers are shown as grey vertical lines. b, The L1 and L2 loop regions and the F and G helices that bind to ssDNA are coloured and numbered as in a, with the rest of each RecA structure omitted for clarity. The ssDNA is numbered starting with the 5'-most nucleotide in each nucleotide triplet. The 5'-most and 3'-most nucleotide triplets have only two and one ordered nucleotides, respectively. Portions of the L1 and L2 loops of the C-terminal RecA are disordered (dashed lines).

Chen, Yang & Pavletich, 2008, Nature 453, 489-484

Crystal structure of RecA nucleoprotein filaments

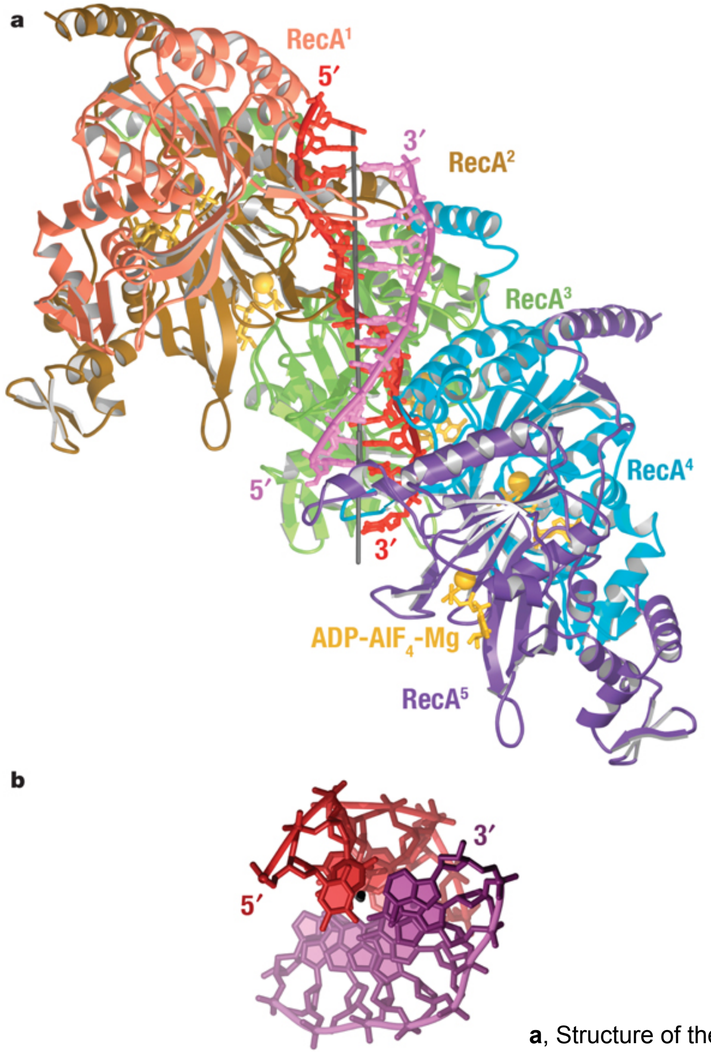

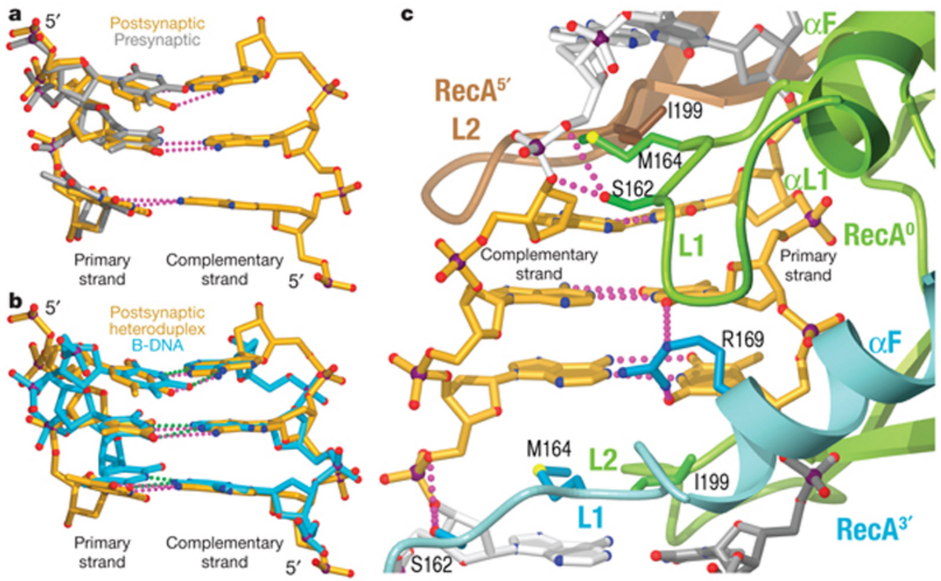

a, Superposition of the presynaptic nucleotide triplet (grey) and postsynaptic base-pair triplet (yellow). Watson–Crick hydrogen bonds are indicated by dotted lines (magenta). The two strands of the postsynaptic base-pair triplet can be superimposed with a 1.2 Å r.m.s.d. in the positions of all phosphate and ribose atoms. **b**, Superposition of the postsynaptic base-pair triplet (yellow) and B-type DNA (cyan). Watson–Crick hydrogen bonds are shown as dotted lines, coloured magenta for the heteroduplex and green for B-DNA. **c**, Close-up view of the RecA–heteroduplex interface coloured as in Fig 2, showing all the contacts to the complementary strand. The primary strand contacts that differ from the presynaptic state are also shown; the rest are omitted for clarity.

a, Structure of the $RecA_5$–$(ADP\text{-}AlF_4\text{-}Mg)_5$–$(dT)_{15}$–$(dA)_{12}$ complex. The five RecA protomers are coloured as the first five protomers of Fig. 1a. The primary $(dT)_{15}$ strand (red) has 13 ordered nucleotides, and the complementary $(dA)_{12}$ strand (magenta) has 10 ordered nucleotides. **b**, View of the heteroduplex looking down the filament axis, showing the three central base-pair triplets (of $RecA^2$, $RecA^3$ and $RecA^4$).

Chen, Yang & Pavletich, 2008, Nature 453, 489-484

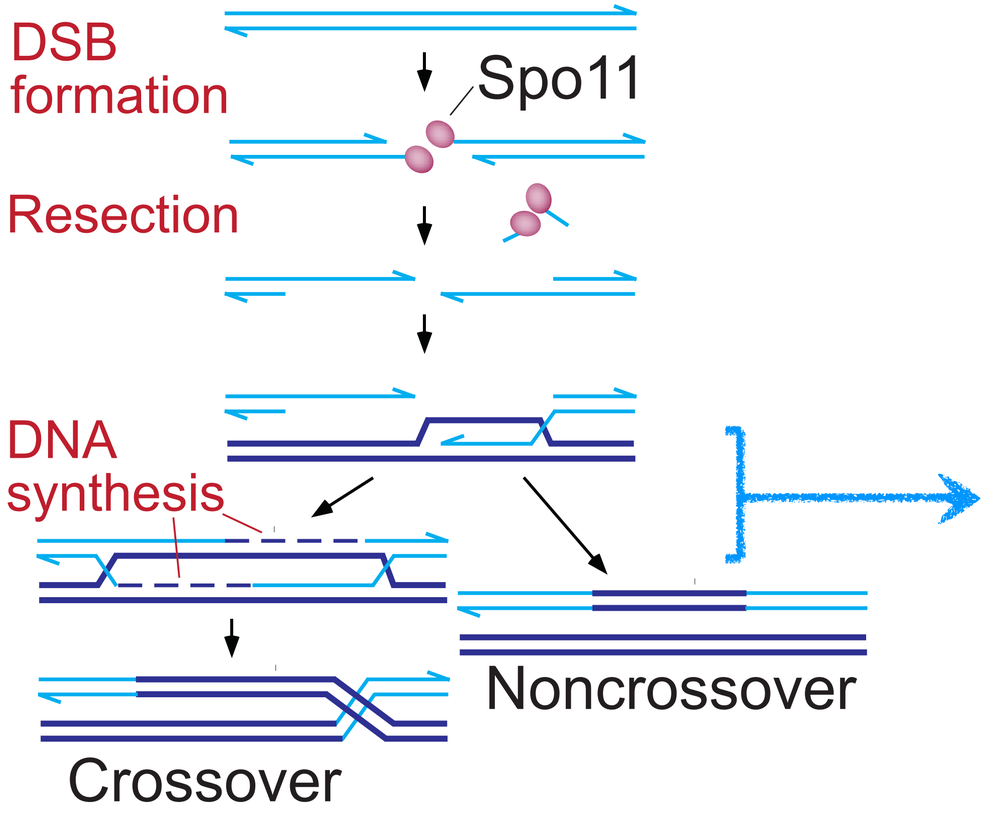

DNA synthesis

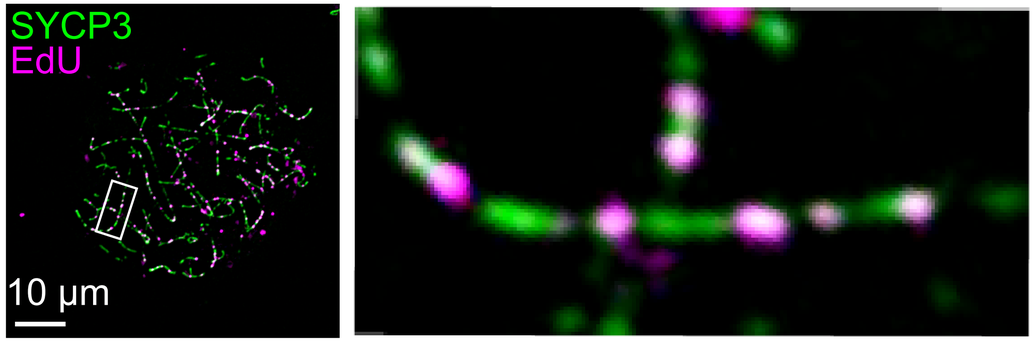

EdU labeling in primary spermatocyte cultures (Yuichiro Saito)

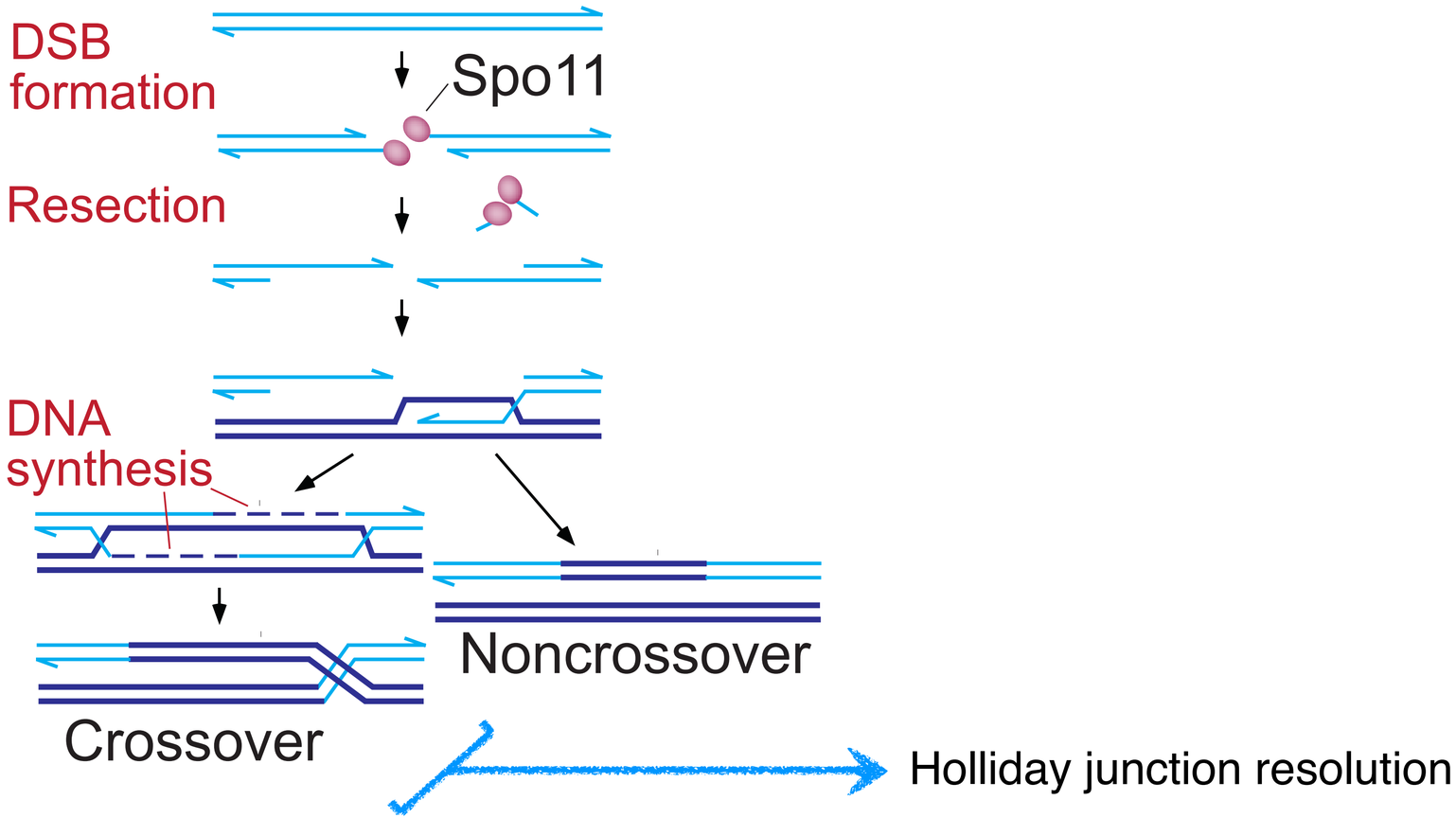
DSB
formation
Spo11
Resection
DNA
synthesis
Noncrossover
Crossover
Holliday junction resolution

Resolution of HJs in fractionated E. coli extracts

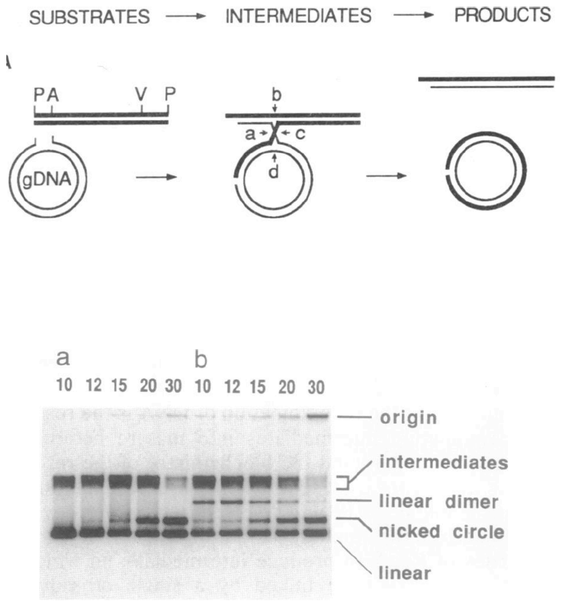

FIG. 1. Resolution of strand-exchange intermediates by fraction V. A 110-μl reaction mixture containing 5.8 μM gapped øX174 DNA and 2.6 μM RecA was incubated for 5 min at 37°C. ^{32}P-labeled linear duplex øX174 DNA (4.5 μM) was added to initiate strand exchange and incubation was continued. At the indicated times (in min after addition of the linear DNA), 10-μl samples were removed and processed in one of two ways. Reactions were stopped (*a*) or supplemented with 7.2 μg of fraction V (FV) and incubation was continued for 5 min (*b*). Reactions were then stopped as above. DNA products were analyzed by 0.7% agarose gel electrophoresis and autoradiography.

Connolly and West (1990) PNAS 87: 8476
Connolly et al. (1991) PNAS 88: 6063

RuvC alters HJ structure upon binding it

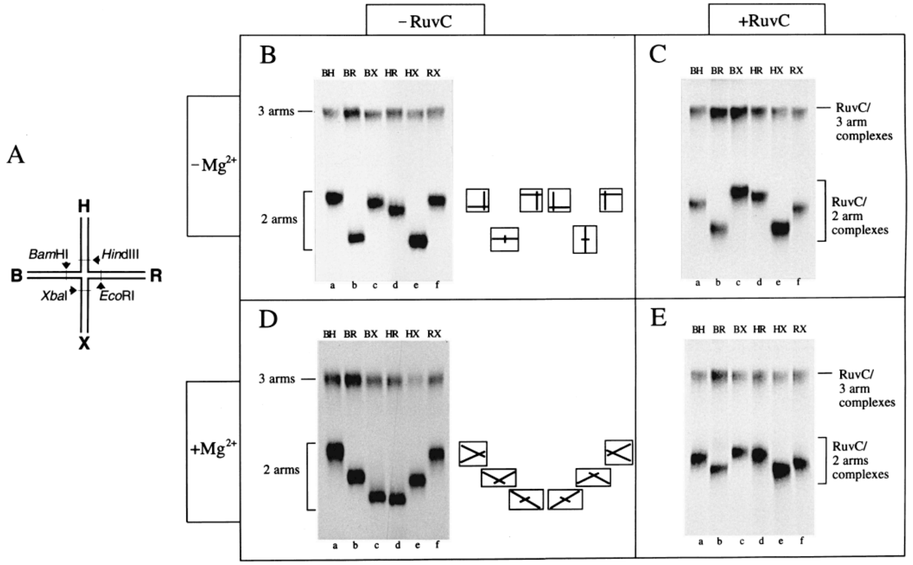

Figure 3. Gel electrophoretic analysis of the configuration of the arms of the Holliday junction in the absence and presence of RuvC protein. The six DNA species produced by digestion with pairwise combinations of restriction enzymes were analysed by electrophoresis through 8% or 10% polyacrylamide gels, either without (B and D) or with RuvC (C and E). Electrophoresis was carried out in the presence of 2 mM EDTA (B and C) or 0.5 mM $MgCl_2$ (D and E). Partially digested junctions (i.e. containing three intact arms) are indicated. The letters (BH, BR, etc.) above each lane indicate the DNA arms that are intact (i.e. long) after restriction enzyme cleavage. A, Schematic of the Holliday junction used in these experiments. The junction was constructed from four 80 nt oligonucleotides such that it contained a unique restriction site in each arm. This junction was cleaved with restriction enzymes in pairwise combinations to generate six unique species. The junction arms are labelled according to the restriction site present in that arm. B, In the presence of EDTA, the six protein-free DNA species produce a 4:2 pattern indicative of the unfolded square structure formed in the absence of cations. The structure of the six species, as implied from their mobilities, is shown on the right. C, Binding of RuvC in the presence of EDTA alters the electrophoretic pattern from that seen in the absence of protein (B), although the junction remains unfolded (4:2 pattern). D, In the presence of Mg^{2+} cations, the protein-free DNA species migrate in a 2:2:2 pattern characteristic of the stacked X-structure with B on X coaxial stacking. The predicted structures of the six species are shown to the right of the gel. E, The six junction species bound by RuvC in the presence of Mg^{2+} no longer migrate with the 2:2:2 pattern characteristic of the folded junction. Instead, the relative mobilities indicate a structure that resembles the unfolded structure seen in the absence of cations (C).

Bennett & West (1995) J Mol Biol 252: 213.

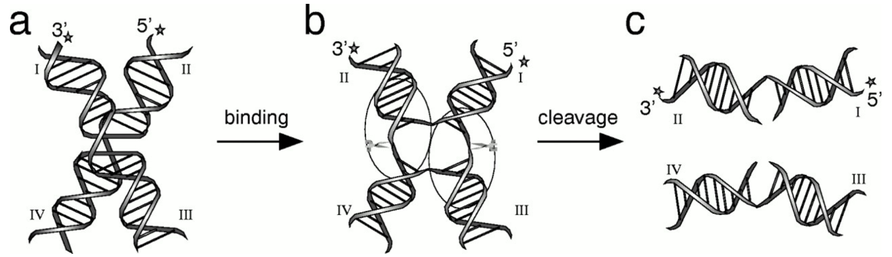

West (1997) Ann. Rev. Genet. 31: 213-244.

Structure-specific nucleases and junction resolution

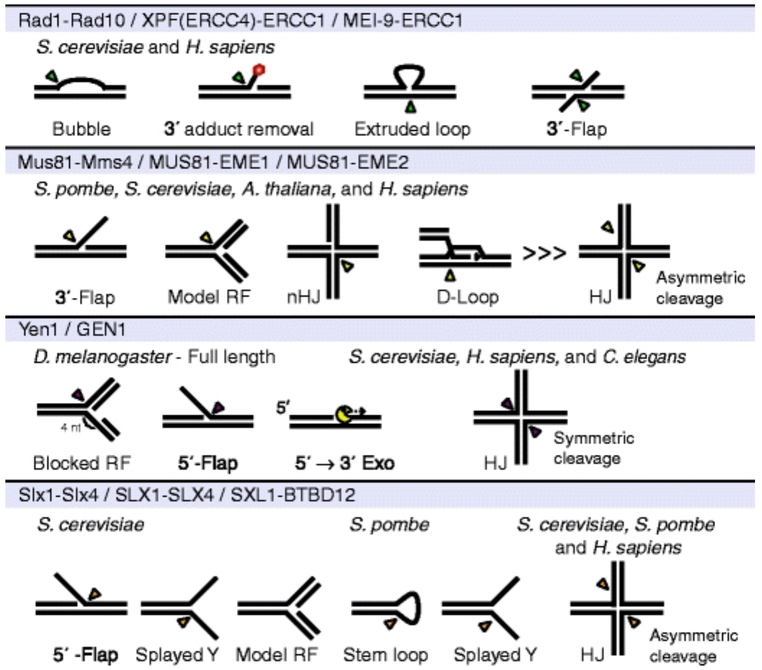

Substrate specificity of eukaryotic structure-selective junction endonucleases. Mapped incision sites for Rad1 (green triangles), Mus81 (yellow triangles), Yen1/GEN1 (purple triangles), and Slx1–Slx4 (orange triangles) are indicated. The incision sites for Slx4 on replication forks have not been mapped and are therefore not represented. D-Loop, displacement loop; nHJ, nicked Holliday junction; RF, replication fork; NER, nucleotide excision repair; SSA, single-strand annealing; Model RF, model replication fork; Exo, exonuclease activity
Schwartz & Heyer, 2011, Chromosoma 120: 109-127

Double-Holliday junction **dissolution**

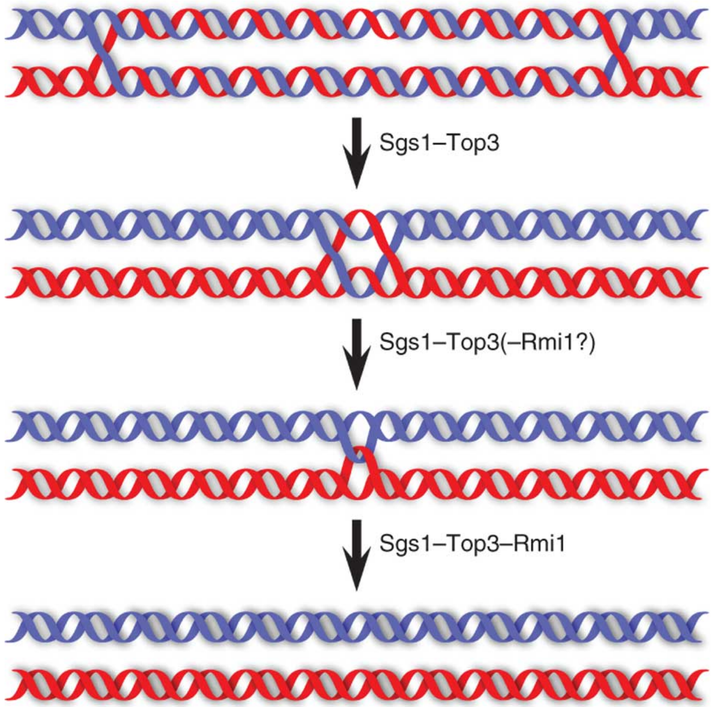

Sgs1 and Top3 catalyze convergent HJ migration. Rmi1 is likely an integral part of the Sgs1–Top3 complex, but its function is dispensable during this initial branch migration phase, although it may become important in later steps of this phase. Rmi1 stimulates dHJ dissolution when both junctions are in close proximity. Rmi1 subsequently stimulates the decatenation of a hemicatenane, the last anticipated intermediate of dHJ dissolution.
Cejka et al., 2010, Nat Struct & Molecular Biol. 17: 1377-1382

Article | Published: 19 August 2020

PCNA activates the MutLγ endonuclease to promote meiotic crossing over

Dhananjaya S. Kulkarni, Shannon N. Owens, Masayoshi Honda, Masaru Ito, Ye Yang, Mary W. Corrigan, Lan Chen, Aric L. Quan & Neil Hunter

Nature **586**, 623–627 (2020) | Cite this article

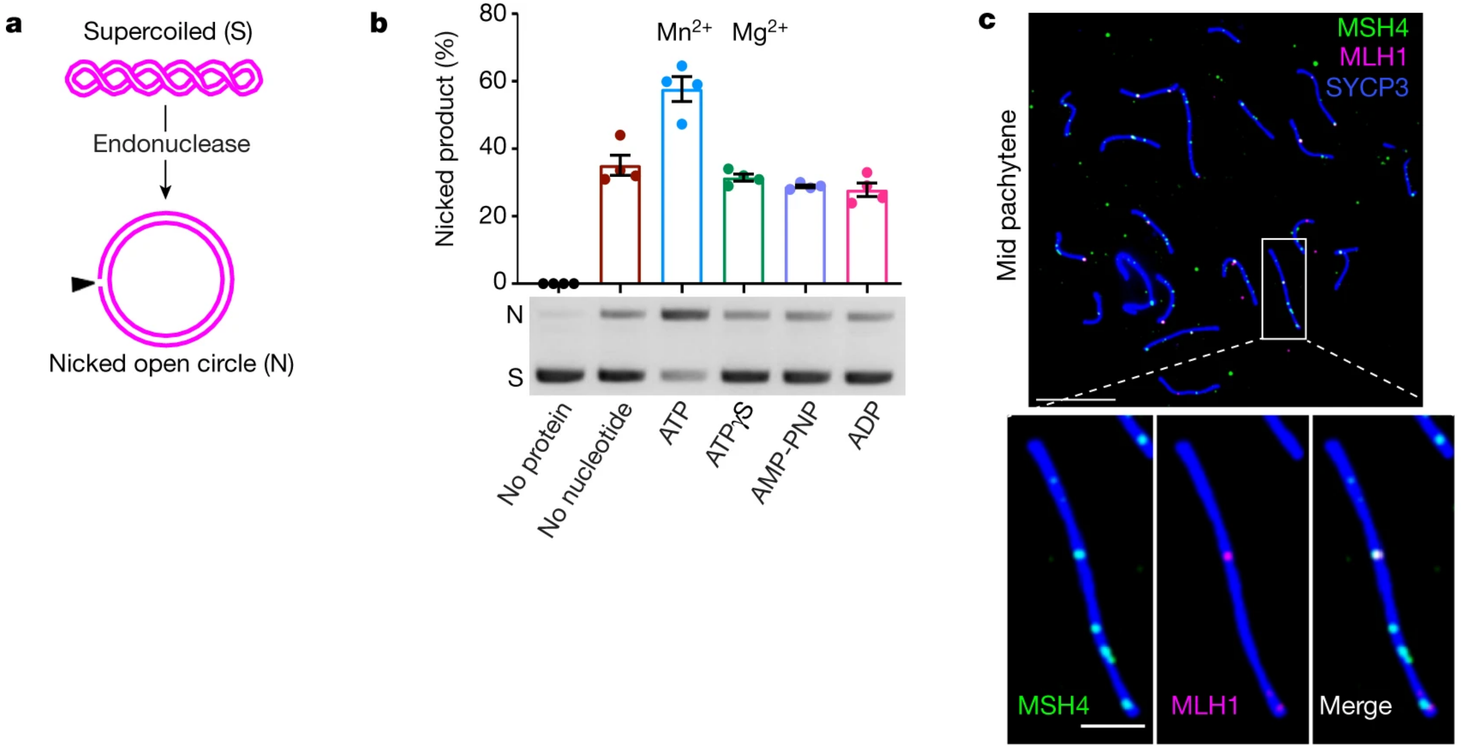

Article | Published: 19 August 2020

Regulation of the MLH1–MLH3 endonuclease in meiosis

Elda Cannavo, Aurore Sanchez, Roopesh Anand, Lepakshi Ranjha, Jannik Hugener, Céline Adam, Ananya Acharya, Nicolas Weyland, Xavier Aran-Guiu, Jean-Baptiste Charbonnier, Eva R. Hoffmann, Valérie Borde, Joao Matos & Petr Cejka

Nature **586**, 618–622 (2020) | Cite this article


My favorite of all
GENESIS
GV60
PEPE AUTO GROUP
NEW YORK
SPO-11
EXCELSIOR
GENESIS OF WHITE PLAINS